Inventory of Supplementary Materials:

Figure S1

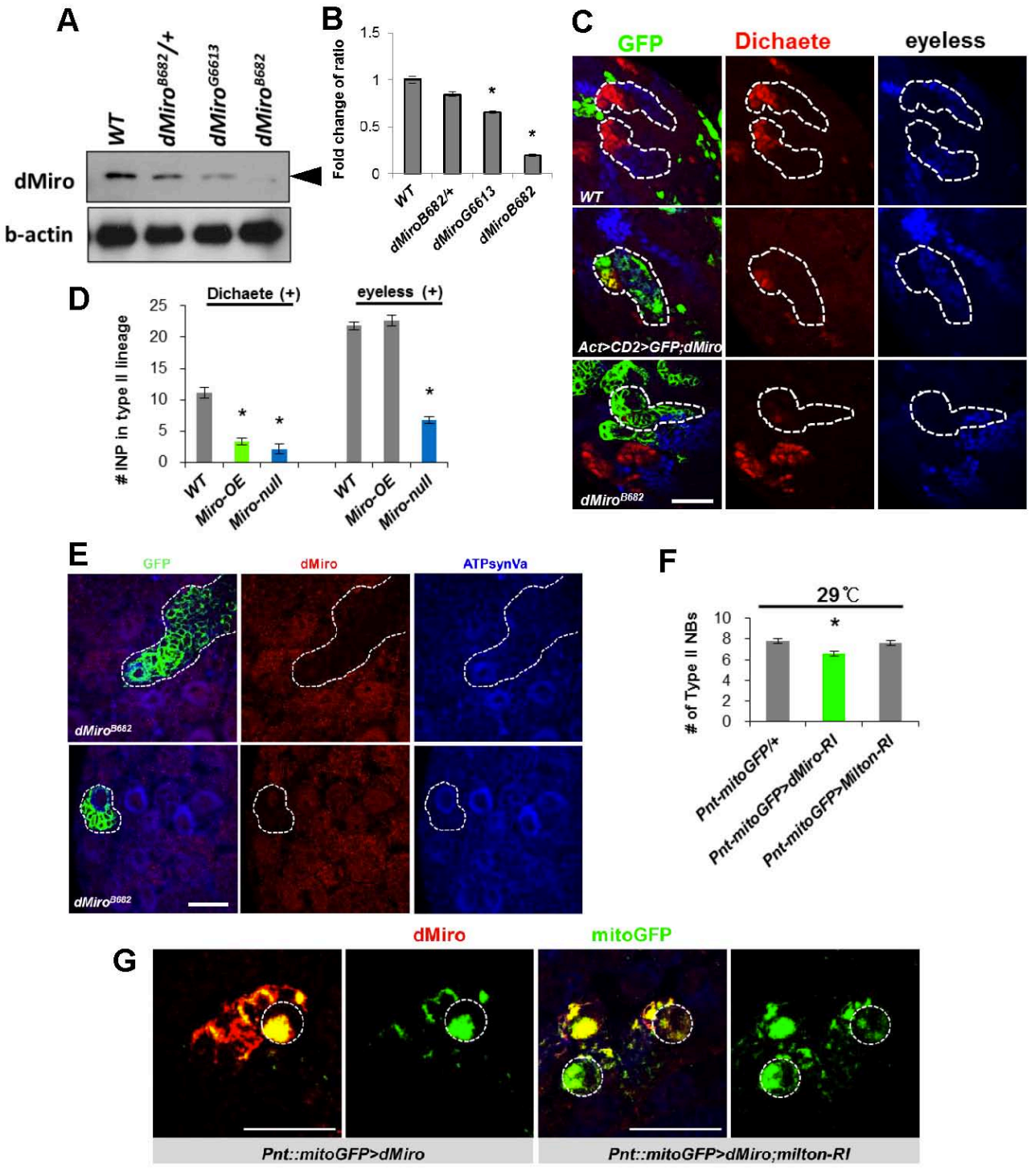
A
WT
dMiroB682/+
dMiroG6613
dMiroB682
dMiro
b-actin
B
Fold change of ratio
1.5
1
0.5
0
WT
dMiroB682/+
dMiroG6613
dMiroB682
C
GFP
Dichaete
eyeless
WT
Act>CD2>GFP;dMiro
dMiroB682
D
Dichaete (+)
eyeless (+)
INP in type II lineage
25
20
15
10
5
0
WT
Miro-OE
Miro-null
WT
Miro-OE
Miro-null
E
GFP
dMiro
ATPsynVa
dMiroB682
dMiroB682
F
29℃
# of Type II NBs
10
8
6
4
2
0
Pnt-mitoGFP/+
Pnt-mitoGFP>dMiro-RI
Pnt-mitoGFP>Milton-RI
G
dMiro
mitoGFP
Pnt::mitoGFP>dMiro
Pnt::mitoGFP>dMiro;milton-RI

Figure S1, Related to Figure 1. Analysis of Miro Function in Fly NBs

(A) WB analysis showing lack of dMiro protein expression in *dMiro*^{B682} mutant. Actin serves as loading control.

(B) Quantification of dMiro protein level from A.

(C) Immunostaining and quantification of D-positive young IPs (Red) and Ey-positive old IPs (Blue) in *dMiro* mutant MARCM clones or Flip-out dMiro OE clones in larval brain. Clones were visualized with GFP marker and the type II NB lineages are outlined with white dashed line.

(D) Quantification of the number of young (D+) or old (Ey+) IPs from C.

(E) Immunostaining showing lack of effect on mitochondrial morphology by *dMiro* mutation in type II (upper panels) or type I (lower panels) NB clones. Clones were visualized with GFP marker and the NB lineages are outlined with white dashed line. dMiro staining verifies lack of dMiro expression in mutant clones and ATPsynVa staining shows mitochondrial morphology.

(F) Quantification showing effects of *dMiro* or *Milton* RNAi on type II NB number. Animals were raised at 29^{o}C to enhance RNAi efficiency.

(G) Knockdown of Milton rescued abnormal mitochondrial distribution caused by dMiro OE in larval brain NBs. Circles with white dashed line mark the NBs of interest. Error bar, SEM; *, $P<0.05$ in Student's *t*-tests. Scale bars, 20 μm.

Figure S2

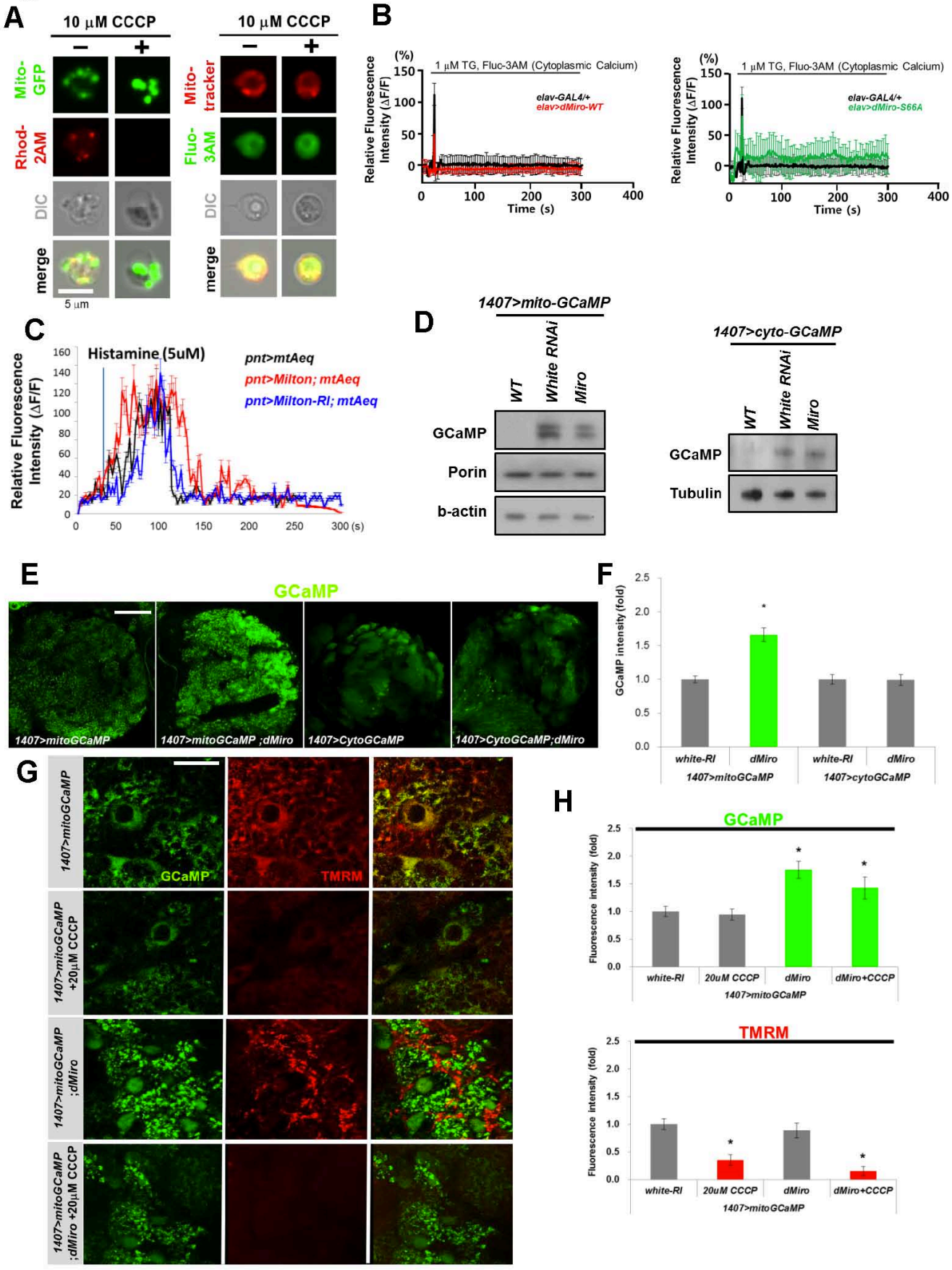
A
10 μM CCCP
10 μM CCCP
Mito-GFP
Rhod-2AM
DIC
merge
Mito-tracker
Fluo-3AM
DIC
merge
5 μm
B
1 μM TG, Fluc-3AM (Cytoplasmic Calcium)
elav-GAL4/+
elav>dMiro-WT
Relative Fluorescence Intensity (ΔF/F)
Time (s)
1 μM TG, Fluo-3AM (Cytoplasmic Calcium)
elav-GAL4/+
elav>dMiro-S66A
C
Histamine (5uM)
pnt>mtAeq
pnt>Milton; mtAeq
pnt>Milton-Rl; mtAeq
Relative Fluorescence Intensity (ΔF/F)
D
1407>mito-GCaMP
WT
White RNAi
Miro
GCaMP
Porin
b-actin
1407>cyto-GCaMP
WT
White RNAi
Miro
GCaMP
Tubulin
E
GCaMP
1407>mitoGCaMP
1407>mitoGCaMP ;dMiro
1407>CytoGCaMP
1407>CytoGCaMP;dMiro
F
GCaMP intensity (fold)
white-Rl
dMiro
white-Rl
dMiro
1407>mitoGCaMP
1407>cytoGCaMP
G
1407>mitoGCaMP
GCaMP
TMRM
1407>mitoGCaMP +20μM CCCP
1407>mitoGCaMP ;dMiro
1407>mitoGCaMP ;dMiro +20μM CCCP
H
GCaMP
Fluorescence intensity (fold)
white-Rl
20uM CCCP
dMiro
dMiro+CCCP
1407>mitoGCaMP
TMRM
Fluorescence intensity (fold)
white-Rl
20uM CCCP
dMiro
dMiro+CCCP
1407>mitoGCaMP

Figure S2, Related to Figure 2. Analyses of the Effects of Miro on Ca^{2+}_{mito} Homeostasis

(A) Evidence that Rhod-2 AM specifically monitors mitochondrial Ca^{2+}. In primary *Drosophila* neuronal culture, Rhod-2 AM signal overlaps extensively with the mitochondrial marker mito-GFP. Depolarization of mitochondrial membrane potential with CCCP abolished Rhod-2AM signal without affecting cytosolic Ca^{2+} signal monitored with Fluo-3 AM fluorescence, thus validating the specificity of Rhod-2 AM in monitoring mitochondrial Ca^{2+}.

(B) Effects of pan-neuronal *elav-Gal4* driven dMiro-WT or dMiro-S66A on TG-stimulated elevation of cytosolic Ca^{2+} as measured with Fluo-3 AM fluorescence in primary cultured fly neurons. The traces show mean response of cells present in the microscope field and are representative of more than 3 experiments.

(C) Lack of effect of Milton OE or RNAi on Ca^{2+}_{mito} as monitored with genetically-encoded mito-AEQ. The traces show mean response of 10 dissected larval brains present in the microtiter plate and are representative of more than 3 tests.

(D) WB analysis with anti-GFP quantifying mito-GCaMP and cytosolic GCaMP protein levels in 3rd instar larva brain expressing Miro or a control *white RNAi* transgene. Porin serves as mitochondrial marker and actin or tubulin serve as loading controls.

(E, F) *In vivo* Ca^{2+} imaging showing that NB-specific dMiro-OE altered basal mitochondrial calcium level (monitored with mito-GCaMP), but not cytosolic calcium level (monitored with cyto-GCaMP). (F) Quantification of normalized GCaMP intensity from E.

(G) NB-specific dMiro-OE altered mitochondrial calcium level without changing mitochondrial membrane potential as measured with TMRM. TMRM signals were dramatically reduced by CCCP treatment, which causes mitochondrial depolarization, indicating specificity of this dye staining.

(H) Quantification showing normalized Ca^{2+}_{mito} (mito-GCaMP) and mitochondrial membrane potential (TMRM) fluorescence signals from G.

Error bar, SEM; *, $P<0.05$ in Student's *t*-tests. Scale bars, 20 μm (A, G), 100 μm (E).

Figure S3

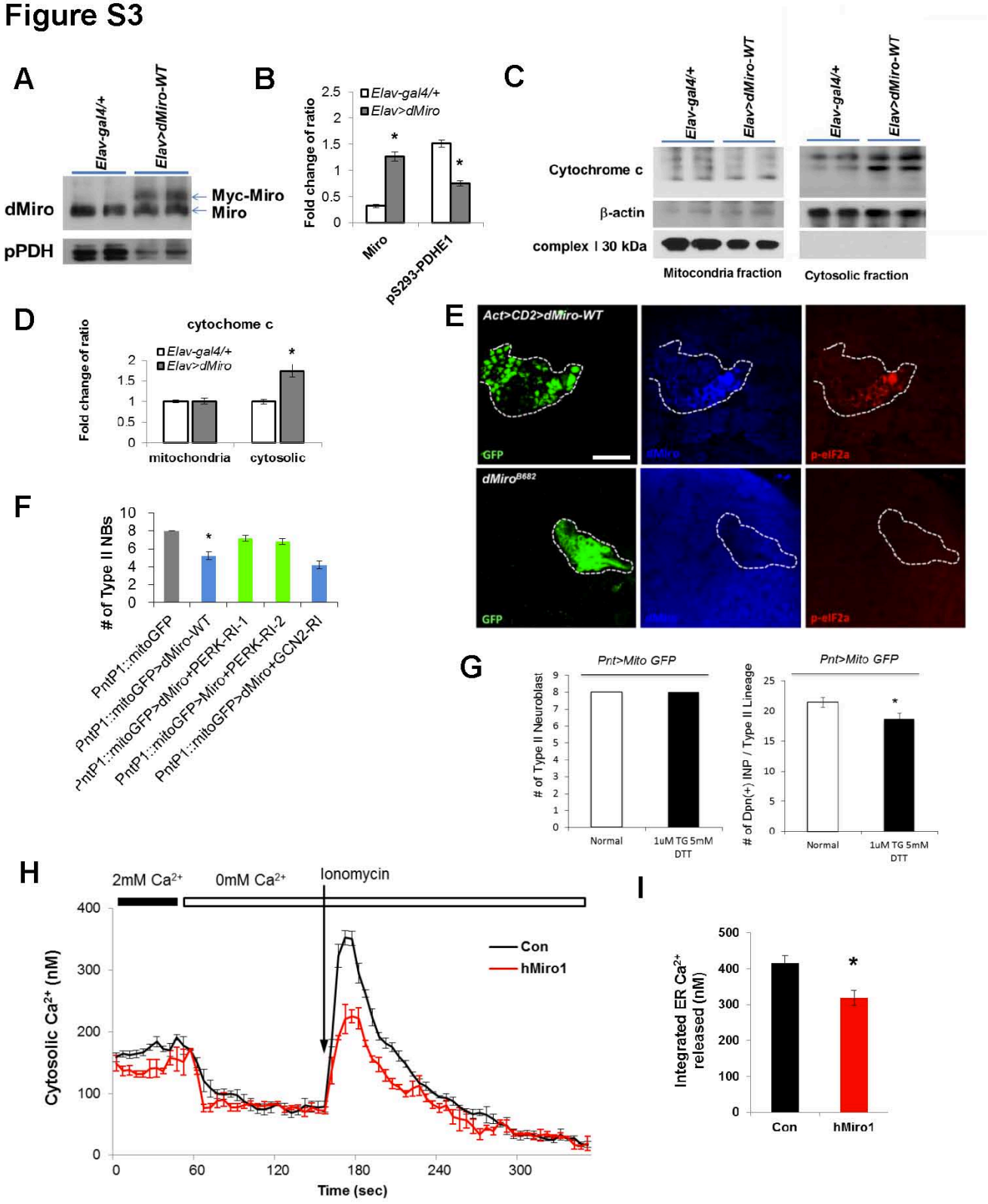
A
Elav-gal4/+
Elav>dMiro-WT
dMiro
Myc-Miro
Miro
pPDH
B
Elav-gal4/+
Elav>dMiro
Fold change of ratio
Miro
pS293-PDHE1
C
Elav-gal4/+
Elav>dMiro-WT
Cytochrome c
β-actin
complex I 30 kDa
Mitocondria fraction
Cytosolic fraction
D
cytochome c
Elav-gal4/+
Elav>dMiro
Fold change of ratio
mitochondria
cytosolic
E
Act>CD2>dMiro-WT
GFP
dMiro
p-eIF2a
dMiroB682
F
# of Type II NBs
PntP1::mitoGFP
PntP1::mitoGFP>dMiro-WT
PntP1::mitoGFP>dMiro+PERK-RI-1
PntP1::mitoGFP>Miro+PERK-RI-2
PntP1::mitoGFP>dMiro+GCN2-RI
G
Pnt>Mito GFP
# of Type II Neuroblast
Normal
1uM TG 5mM DTT
# of Dpn(+) INP / Type II Lineage
H
2mM Ca2+
0mM Ca2+
Ionomycin
Con
hMiro1
Cytosolic Ca2+ (nM)
Time (sec)
I
Integrated ER Ca2+ released (nM)
Con
hMiro1

Figure S3, Related to Figure 3. Analyses of the Effects of Miro on Mitochondrial Function

(A, B) WB analysis showing reduced p-PDHE1 level in dMiro-OE fly brain extract. Note that the level of transgenic Miro is not exceeding endogenous Miro level. B, quantification of the levels of dMiro and phosphorylated PDHE1 in control *Elav-Gal4/+* and *Elav>dMiro-OE* samples from A.

(C, D) WB analysis showing the release of cyt C into the cytosol in dMiro-OE animal brain. Complex I 30 kD and β-actin were used as markers for mitochondrial and cytosolic fractions, respectively. D, quantification of the levels of cyt C from C.

(E) Immunostaining of p-eIF2α, an ER stress marker, in dMiro-OE Flip-out clones or $dMiro^{B682}$ mutant MARCM clones. Clones were visualized with a GFP marker and outlined with white dashed lines.

(F) Genetic interaction studies showing rescue of dMiro OE-induced NB loss by RNAi of a candidate eIF2α kinase PERK, but not GCN2. Two independent PERK RNAi lines showed the same effect.

(G) ER stress-inducing chemicals (DTT + TG) had no obvious effect on the number of type II NB but reduced the number of Dpn-positive IPs.

(H) Estimating ER Ca^{2+} level by measuring ionomycin-releasable Ca^{2+} content from intracellular stores in hMiro1 transfected HeLa cells. Representative Ca^{2+} traces following emptying of ER stores with 5 μM ionomycin in HeLa cells with or without hMiro1 transfection are shown. Cells were cultured in low Ca^{2+} media (100 μM) after transfection, following by a 30-min incubation in normal Ca^{2+} (2 mM) immediately before calcium imaging to allow restoration of ER calcium. (I) Quantification showing integrated release of $Ca2^{+}$ from intracellular stores in hMiro1 transfected cells within 2 min after ionomycin treatment. Error bar: SEM; *, $p<0.05$ in Student's *t*-tests. Scale bars, 20 μm.

Figure S4

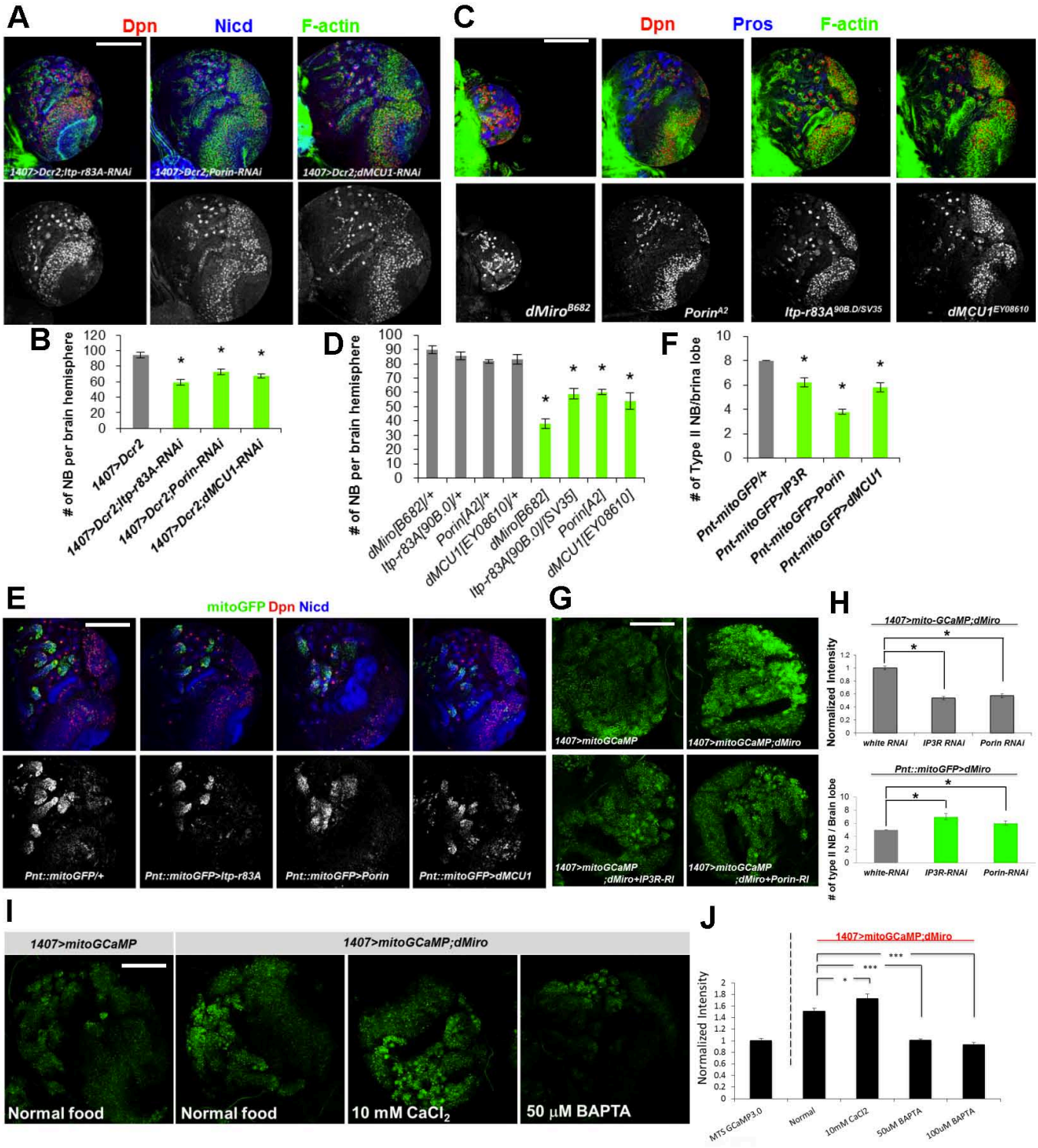
A
Dpn
Nicd
F-actin
1407>Dcr2;Itp-r83A-RNAi
1407>Dcr2;Porin-RNAi
1407>Dcr2;dMCU1-RNAi
C
Dpn
Pros
F-actin
dMiro^B682
Porin^A2
Itp-r83A^90B.D/SV35
dMCU1^EY08610
B
# of NB per brain hemisphere
1407>Dcr2
1407>Dcr2;Itp-r83A-RNAi
1407>Dcr2;Porin-RNAi
1407>Dcr2;dMCU1-RNAi
D
# of NB per brain hemisphere
dMiro[B682]/+
Itp-r83A[90B.0]/+
Porin[A2]/+
dMCU1[EY08610]/+
dMiro[B682]
Itp-r83A[90B.0]/[SV35]
Porin[A2]
dMCU1[EY08610]
F
# of Type II NB/brina lobe
Pnt-mitoGFP/+
Pnt-mitoGFP>IP3R
Pnt-mitoGFP>Porin
Pnt-mitoGFP>dMCU1
E
mitoGFP Dpn Nicd
Pnt::mitoGFP/+
Pnt::mitoGFP>Itp-r83A
Pnt::mitoGFP>Porin
Pnt::mitoGFP>dMCU1
G
1407>mitoGCaMP
1407>mitoGCaMP;dMiro
1407>mitoGCaMP ;dMiro+IP3R-RI
1407>mitoGCaMP ;dMiro+Porin-RI
H
1407>mito-GCaMP;dMiro
Normalized Intensity
white RNAi
IP3R RNAi
Porin RNAi
Pnt::mitoGFP>dMiro
# of type II NB / Brain lobe
white-RNAi
IP3R-RNAi
Porin-RNAi
I
1407>mitoGCaMP
1407>mitoGCaMP;dMiro
Normal food
Normal food
10 mM CaCl2
50 μM BAPTA
J
1407>mitoGCaMP;dMiro
Normalized Intensity
MTS GCaMP3.0
Normal
10mM CaCl2
50uM BAPTA
100uM BAPTA

Figure S4, Related to Figure 4. Additional Analysis of the Function of ER-Mitochondria Ca^{2+} Transfer-Related Genes in NB Maintenance

(A, B) RNAi of fly IP3R, Porin, or MCU resulted in reduced NB number in the larval brain. B, quantification of NB number shown in A.

(C, D) Homozygous mutants of *dMiro*, *Porin*, *IP3R*, or *MCU* show reduced NB number in third instar larval brain. D, quantification of NB number shown in C. Larval brains were immunostained for Dpn, Nicd, and F-actin in **A** or Dpn, Pros, and F-actin in **C**. Dpn only signal is shown in the lower panels in **A** and **C**.

(E, F) IP3R, Porin, or MCU overexpression driven by *Pnt-Gal4* in type II NB lineages led to reduced NB number. Type II NBs are marked by a co-expressed mito-GFP marker and also stained for Dpn and Nicd. Dpn only signal is shown in the lower panels in E. F, quantification of type II NB number shown in E.

(G, H) Increased basal mitochondrial calcium level (mito-GCaMP signal) induced by dMiro OE was reduced by RNAi-mediated knockdown of ERMCS components IP3R and Porin. H, quantification of normalized GCaMP intensity from G, and effect of IP3R RNAi and Porin RNAi on dMiro OE induced type II NB loss.

(I, J) Response of mitochondrial calcium level to exogenous calcium ($CaCl_2$) and calcium chelator (BAPTA) in 3rd instar larva brains. $CaCl_2$ and BAPTA were supplemental to normal fly food. J, quantification of normalized GCaMP intensity from I.

Error bar, SEM; *, $P<0.05$ in Student's *t*-tests. Scale bars, 100 μm.

Figure S5

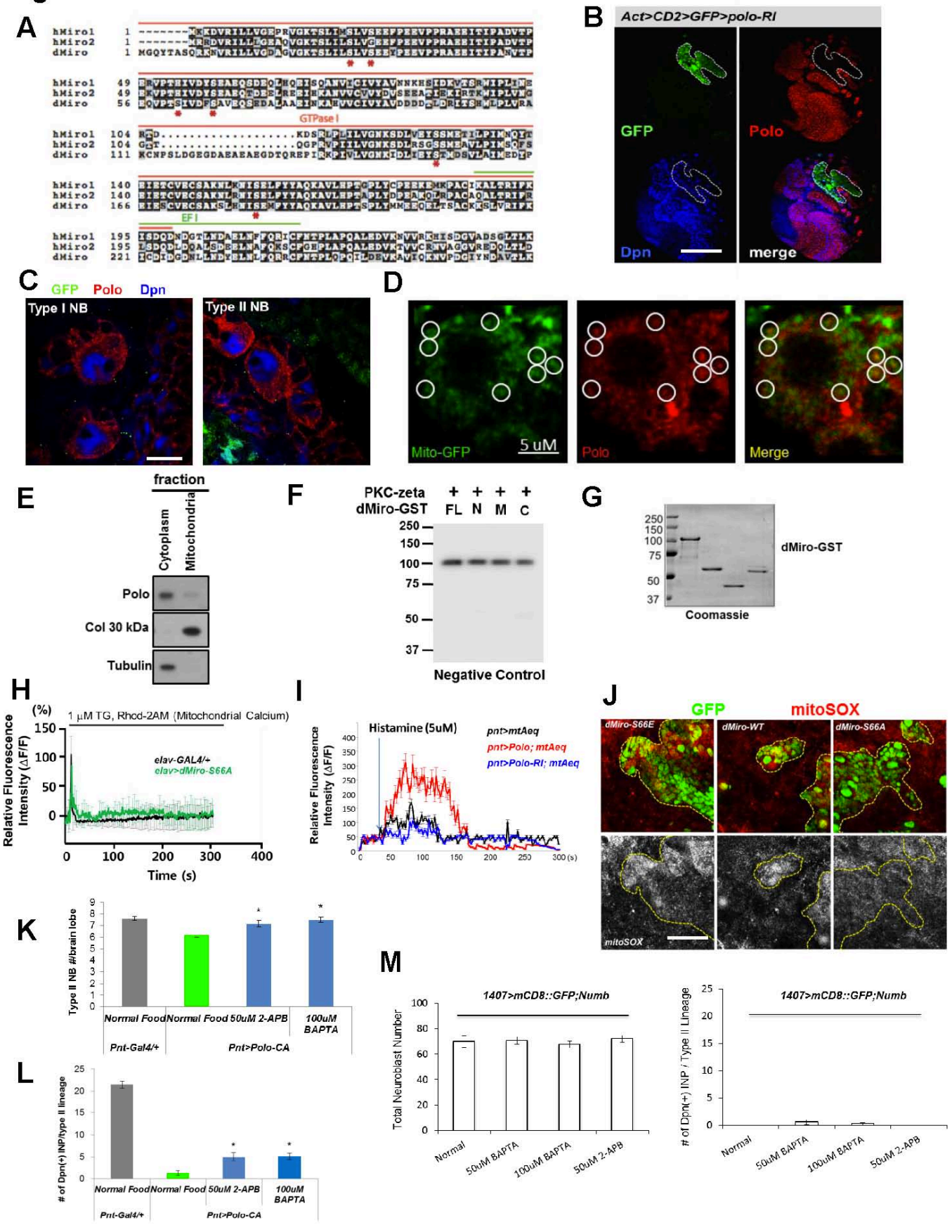
A
hMiro1
hMiro2
dMiro
GTPase I
EF I
B
Act>CD2>GFP>polo-RI
GFP
Polo
Dpn
merge
C
GFP Polo Dpn
Type I NB
Type II NB
D
Mito-GFP
5 uM
Polo
Merge
E
fraction
Cytoplasm
Mitochondria
Polo
Col 30 kDa
Tubulin
F
PKC-zeta + + + +
dMiro-GST FL N M C
250
150
100
75
50
37
Negative Control
G
250
150
100
75
50
37
dMiro-GST
Coomassie
H
(%)
1 μM TG, Rhod-2AM (Mitochondrial Calcium)
Relative Fluorescence Intensity (ΔF/F)
elav-GAL4/+
elav>dMiro-S66A
Time (s)
I
Histamine (5uM)
pnt>mtAeq
pnt>Polo; mtAeq
pnt>Polo-RI; mtAeq
Relative Fluorescence Intensity (ΔF/F)
J
GFP
mitoSOX
dMiro-S66E
dMiro-WT
dMiro-S66A
mitoSOX
K
Type II NB #/brain lobe
Normal Food
Normal Food
50uM 2-APB
100uM BAPTA
Pnt-Gal4/+
Pnt>Polo-CA
L
# of Dpn(+) INP/type II lineage
Normal Food
Normal Food
50uM 2-APB
100uM BAPTA
Pnt-Gal4/+
Pnt>Polo-CA
M
1407>mCD8::GFP;Numb
Total Neuroblast Number
Normal
50uM BAPTA
100uM BAPTA
50uM 2-APB
1407>mCD8::GFP;Numb
# of Dpn(+) INP / Type II Lineage
Normal
50uM BAPTA
100uM BAPTA
50uM 2-APB

Figure S5, Related to Figure 5. Additional Data Showing the Effects of Polo-Miro Signaling on Ca^{2+}_{mito} Homeostasis

(A) Alignment between dMiro and human Miro amino acid sequences showing the position of the conserved Ser residue (marked with *) in the first GTPase domain.

(B) Immunostaining of Polo in Polo-RNAi Flip-out clones validating the specificity of the Polo antibody.

(C) Punctate cytoplasmic staining of Polo in type I and type II NBs of larval brain.

(D) Co-localization between endogenous Polo (red) and the mitochondrial marker mito-GFP (green). Circles mark areas of Polo and mito-GFP colocalization.

(E) WB analysis of subcellular fractions indicates that Polo protein was present in both the cytoplasmic and mitochondrial fractions prepared from 3rd instar larval brains. Complex-I 30 kD subunit and tubulin serve as mitochondrial and cytoplasmic markers, respectively.

(F) Control experiment showing lack of phosphorylation of full-length or fragments of dMiro by PKC-zeta *in vitro*. Autoradiograph is shown. Only kinase autophosphorylation of PKC-zeta was detected.

(G) Coomassie blue staining indicating that equal amounts of GST-Miro fusion proteins were used in F.

(H) Rhod-2 AM staining showing that Miro-S66A OE failed to induce elevated mitochondrial calcium levels. Traces show mean response of cells present in the microscope field and are representative of more than 3 experiments.

(I) Mitochondrial calcium imaging with mito-AEQ showing effects of Polo-OE or Polo-RNAi on Ca^{2+}_{mito} level. The traces show mean response of 10 dissected larval brains present in the microtiter plate and are representative of more than 3 tests.

(J) Mito-SOX staining in Flip-out clones of dMiro-WT, -S66A, -S66E OE NBs. Clones are marked with GFP and outlined with dashed line. Lower panels show Mito-SOX staining only.

(K, L) Quantification showing effects of 2-APB or BAPTA feeding in rescuing the loss of type II NBs and IPs induced by Polo-CA OE.

(M) Quantification showing that the reduction in the numbers of total NBs and Dpn-positive IPs in Numb OE larval brain was not rescued by feeding with BAPTA and 2-APB.

Error bar, SEM; *, $P<0.05$ in Student's *t*-tests. Scale bars, 100 μm (B), 10 μm (C, D), 20 μm (J).

Figure S6

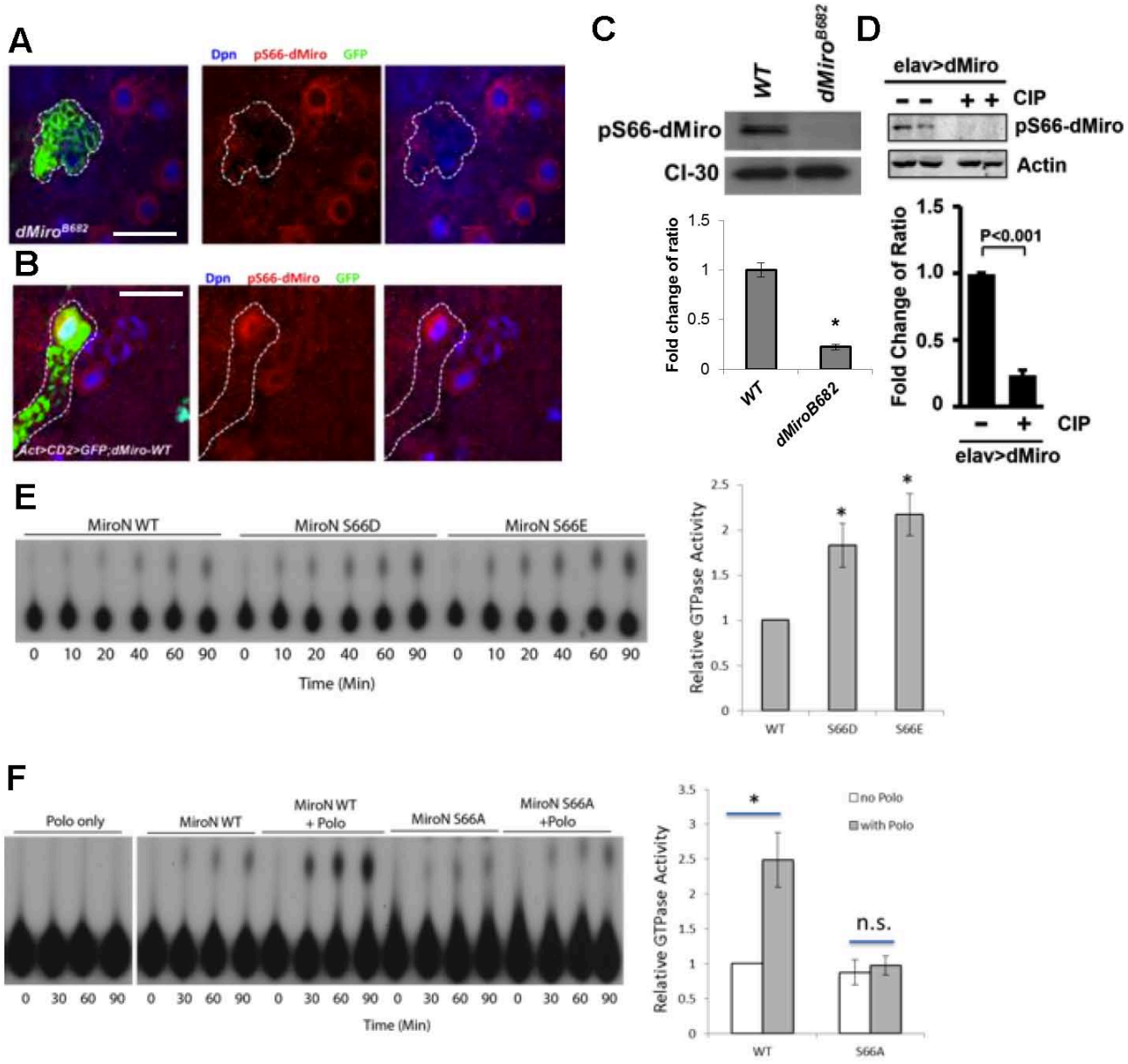
A
Dpn pS66-dMiro GFP
dMiroB682
B
Dpn pS66-dMiro GFP
Act>CD2>GFP;dMiro-WT
C
WT
dMiroB682
pS66-dMiro
CI-30
Fold change of ratio
1.5
1
0.5
0
*
WT
dMiroB682
D
elav>dMiro
- - + + CIP
pS66-dMiro
Actin
Fold Change of Ratio
1.5
1.0
0.5
0
P<0.001
- + CIP
elav>dMiro
E
MiroN WT
MiroN S66D
MiroN S66E
0 10 20 40 60 90 0 10 20 40 60 90 0 10 20 40 60 90
Time (Min)
Relative GTPase Activity
2.5
2
1.5
1
0.5
0
*
*
WT
S66D
S66E
F
Polo only
MiroN WT
MiroN WT + Polo
MiroN S66A
MiroN S66A +Polo
0 30 60 90 0 30 60 90 0 30 60 90 0 30 60 90 0 30 60 90
Time (Min)
Relative GTPase Activity
3.5
3
2.5
2
1.5
1
0.5
0
*
n.s.
no Polo
with Polo
WT
S66A

Figure S6, Related to Figure 6. Additional Data Showing the Effects of Miro Phosphorylation by Polo

(A-C) Immunostaining and WB analyses showing specificity of the p-S66-Miro antibody. p-S66-Miro signal was lost in immunostaining of *dMiro* mutant clones (A) or in WB analysis of *dMiro* mutant brain extracts (C), but increased in immunostaining of dMiro OE NBs (B). NB clones are marked with GFP expression and outlined with dashed lines.

(D) WB analysis showing that the pS66-Miro signal is sensitive to phosphatase treatment. Protein extract prepared from *elav-Gal4>dMiro-OE* was mocked-treated or treated with calf intestinal alkaline phosphatase (CIP) and subjected to WB analysis. Bar graph shows data quantification.

(E) *In vitro* GTPase assays showing that phospho-mimetic dMiro possesses increased GTPase activity.

(F) *In vitro* GTPase assays showing that prior phosphorylation of dMiro-WT, but not dMiro-S66A, with PLK1 resulted in increased GTPase activity.

Error bar, SEM; *, $P<0.05$ in Student's *t*-tests.

Figure S7

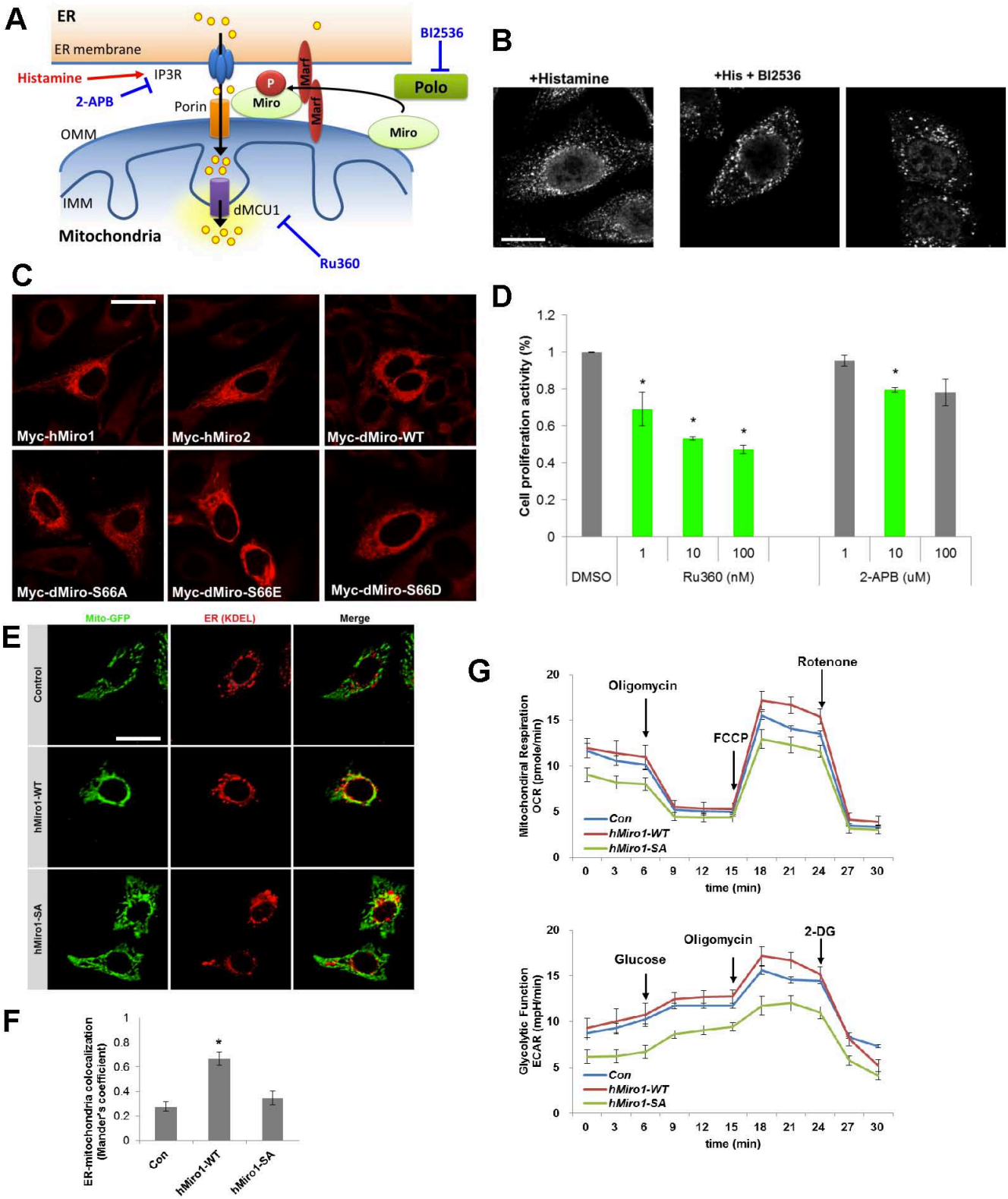
A
ER
ER membrane
Histamine
IP3R
2-APB
Porin
OMM
IMM
Mitochondria
dMCU1
Ru360
BI2536
Polo
P
Miro
Marf
Miro
B
+Histamine
+His + BI2536
C
Myc-hMiro1
Myc-hMiro2
Myc-dMiro-WT
Myc-dMiro-S66A
Myc-dMiro-S66E
Myc-dMiro-S66D
D
Cell proliferation activity (%)
1.2
1
0.8
0.6
0.4
0.2
0
DMSO
1
10
100
Ru360 (nM)
1
10
100
2-APB (uM)
E
Mito-GFP
ER (KDEL)
Merge
Control
hMiro1-WT
hMiro1-SA
F
ER-mitochondria colocalization (Mander's coefficient)
1
0.8
0.6
0.4
0.2
0
Con
hMiro1-WT
hMiro1-SA
G
Mitochondiral Respiration OCR (pmole/min)
Oligomycin
FCCP
Rotenone
Con
hMiro1-WT
hMiro1-SA
0 3 6 9 12 15 18 21 24 27 30
time (min)
Glycolytic Function ECAR (mpH/min)
Glucose
Oligomycin
2-DG
Con
hMiro1-WT
hMiro1-SA
0 3 6 9 12 15 18 21 24 27 30
time (min)

Figure S7, Related to Figure 7. Additional Data Showing the Effects of PLK-Miro Signaling in Mammalian Cells

(A) Diagram of the molecular players at the ERMCS and the targets of the various compounds used in this study.

(B) PLK inhibitor BI2536 reduced the recruitment of hMiro1/Rhot1 to the perinuclear ER area induced by histamine in HeLa cells. Immunostaining for hMiro1 is shown.

(C) Immunostaining showing differential localization patterns of myc-tagged hMiro1, hMiro2, dMiro, and dMiro phospho-variants to the perinuclear ER area in cultured HeLa cells. Immunostaining for myc is shown.

(D) Effects of RU360 and 2-APB on mammalian NSC proliferation. Various concentrations of the compounds were used in cell proliferation assays.

(E, F) Immunostaining showing that ER-mitochondria interaction was increased in hMiro1-WT transfected cells comparing with control cells, while ER-mitochondrial interaction did not change in cells transfected with phospho-mutant form of hMiro1 (hMiro1-S59A). F, quantification of mitochondria (Mito-GFP) and ER (KDEL) colocalization using Mander's coefficient evaluation.

(G) Real-time changes in OCR and Glycolytic rate (ECAR) were measured in control and hMiro1-WT or hMiro1-S59A transfected human NSCs using the Seahorse Bioscience XF Analyzer.

Error bar, SEM; *, $P<0.05$ in Student's *t*-tests. Scale bars, 100 μm.

Supplemental Experimental Procedures

Drosophila Genetics

Other *Drosophila* stocks used in this study are: *dMiro*^{B628}, *UAS-dMiro, UAS-dMiro-Myc* (K Zinsmaier); *milton*^{92} (X Wang); *porin*^{A2} (JK Chung); *polo*^{9} and *polo*^{10} (DM Glover); *UAS-Marf* (A Whitworth); *UAS-mito-Apoeaquorin* (SA Davies), *UAS-mito-GCaMP3* (F Kawasaki), *PntP1-Gal4* (YN. Jan); *1407-Gal4* (L. Luo). Other transgenes used are: *Polo-WT, Polo-CA* (J Lipsick); *mitoGFP* (W. Saxton); *Marf-RNAi* (M. Guo); *white-RNAi* (D. Smith); *UAS-Drp1* (H. Bellen); *UAS-yNDI1* (D. Walker). *dMiro -RNAi* (v106683), *Polo RNAi* (v20177), *Porin-RNAi* (v101336), *dMCU1-RNAi (v110781)*, *pdk-RNAi* (v106641) and *Dicer2* (v60008) are from VDRC; *dMiro*^{G6613} (B30172), *Itp-r83A*$^{90B.0}$ (B30737), *Itp-r83A*^{SV35} (B30740), *Df(3L)H99* (B1576), *Itp-r83A-RNAi (B51686)*, *UAS-p35* (B5072), *Milton EY* (B15518), *dMCU1 EY* (B16357), *UAS-GCaMP3.0* (B32116), and other common stocks were obtained from Bloomington *Drosophila* Stock Center (USA). To enhance the efficiency of knock-down, *Dicer2* was coexpressed with *RNAi* transgenes as previously described (Song and Lu, 2011).

Pharmacological Treatments

EDTA/EGTA, BAPTA, 2-APB treatments of adult flies: Newly eclosed adult flies were collected and raised on standard corn meal food mixed with the following reagents: EDTA/EGTA (final concentration 250-1000 μM), BAPTA (final concentration 50-100 μM), 2-APB (final concentration 50-100 μM). Each vial contained 10 flies and was maintained at 25 °C. Drug-containing food was freshly made and replaced every 2-3 days. For the measurements of NB phenotypes (NB size and NB/INP number), flies were mated on drug-containing food and maintained in 25°C. 3rd instar larvae developed in these foods were selected for dissection and immunohistochemical analysis.

Biochemical Assays

To perform the dephosphorylation assay for testing the specificity of p-S66 Miro antibody, 50 frozen fly heads of *elav-GAL4>UAS-dMiro-WT* genotype was collected and homogenized in the CIP-lysis buffer (1x CIP buffer, 50mM Tris–HCl pH 8.0, 0.1% NP40, 150mM NaCl, 10% glycerol and EDTA-free protease inhibitors) and centrifuged at 12,000g for 30 min at 4°C. Supernatant was incubated with CIP (New England Biolabs) for 60 min at 37°C. SDS sample loading buffer was added into the mixture to stop the CIP reaction. Samples were boiled at 100°C for 2 min and subjected to WB analysis. For WB analysis in subcellular fractions, fifty 3rd instar larva brains were dissected and homogenized in HBS buffer, and cytoplasmic and mitochondrial fractions separated as described above. For measuring the level of cytosolic GCaMP and mito-GCaMP proteins, 3rd instar larva brains were dissected and homogenized in lysis buffer and blotted with anti-GFP antibody.

The primary antibodies used for WB were: dMiro (1:1000), p-PDHE1 (1:1000, Millipore), PDHE1 (1:1000, abcam), p-AMPK (1:1000, Cell Signaling), AMPK (1:500, Cell Signaling), cyt *C* (1:100; Invitrogen), p-Thr (1:1000, Sigma), p-Ser (1:2000, Invitrogen), VDAC (1:1000; Cell Signaling), Marf (1:1000, Dr. A Whitworth), IP3R (1:1000; Dr. G Hasan), IP3R (1:1000, Santa Cruz), MCU1 (1:1000; Santa Cruz), Actin (1:1000; Millipore), NDUFS3 (1:10000, MitoScience), Calnexin (1:1000; Novus), dKhc (1:1000, Cytoskeleton), GFP (1:5000, abcam), alpha-tubulin (1:1000, AbD Serotec), Porin (1:1000, Dr. JK Chung), Polo (1:1000, Dr. J Lipsick).

In Vitro GTPase Assay

GST fusion proteins of dMiro-N fragment containing the first GTPase domain were used in the assay. To test the effect of Polo phosphorylation on dMiro GTPase activity, GST-dMiro-N coupled to glutathione agarose beads was first subjected to *in vitro* phosphorylation by PLK1, extensively washed with GTPase assay buffer, before used in the GTPase assay. The GTPase activity of Miro (final concentration of 5 μM) was assayed in 10μl of 20 mM HEPES buffer (pH 7.4) containing 100 mM KCl, 10 mM $MgCl_2$, 5 μM cold GTP, 5 μM GDP, 1 mM DTT in the presence of 18 nM hot GTP (α-^{32}P-labeled

GTP) at 30 °C. At each incubation time, the reaction was quenched by the addition of an equal volume of a stop solution (0.5% SDS, 10 mM EDTA, and 2 mM DTT) and heated at 65 °C for 1 min. One microliter of each reaction was spotted onto a polyethyleneimine-cellulose thin layer chromatography (TLC) plate (Sigma-Aldrich) and resolved in 1 M formic acid and 0.5 M LiCl solution. The TLC plate was then dried and exposed to Kodak BioMax MS Film.

In vivo Ca^{2+} Imaging

For measuring mitochondrial Ca^{2+} with mito-AEQ (apoaequorin), larval brains were dissected from transgenic flies and incubated for 4 h in Schneider's medium containing the cofactor of apoaequorin (2.5 μM coelenterazine). Larval brains were placed in an automated luminometer, and base-line luminescence was measured for at least 30 s before adding the IP3R agonist histamine (5 μM). Real-time luminescence was then continuously measured for 5 min. For measuring background level of intercellular calcium, tissue was discharged by incubating in a lysis buffer (1% Triton X-100, 100mM $CaCl_2$). The relative change in luminescence were determined by calculations of $\Delta F/F_0$ for each time point of each measurement as $(F_i-F_0)/F_0$ X100, where F_0 is the background luminescence without larval brain, and F_i the luminescence value for each time point of each measurement.

For calcium imaging with GCaMP, the pan-NB *1407-Gal4* driver was used to express mitochondria-targeted (*UAS-mito-GCaMP3.0*) (Lutas et al., 2012) or cytosolic (*UAS-GCaMP3.0*) GCaMP in 3rd instar larvae raised at 29°C. After briefly washing the larvae in 1x PBS, brains were dissected and immediately placed on the glass slides for live imaging. Images were taken with a Leica TCS SP5 AOBS confocal microscope equipped with a laser scanner and a 40x oil-immersion objective. Series of z-stack images of the larvae brain (step size of 0.5 μm) were taken (1024x1024 pixel; pinhole 1AU; 1x digital zoom) using the 488 nm excitation argon laser set at 20% output power for GFP signals. The intensity of GFP signals in 10 different NBs were measured in merged images through LAS AF (Leica).

Measurement of cytosolic Calcium $[Ca^{2+}]_c$ and estimation of ER store Ca^{2+} content was performed as previously described (Feng et al., 2010) with minor modification. HeLa cells were plated on coverslips and then transfected with pcDNA-hMiro1 or empty vector before measuring cytosolic Ca^{2+}. Cells were loaded with Fura-2 AM at 1μM in calcium recording buffer (126 mM NaCl, 2 mM $MgCl_2$, 4.5 mM KCl, 10 mM Glucose, 20 mM Hepes pH 7.4, 2 mM $CaCl_2$) or Ca^{2+}-free buffer (No $CaCl_2$ in calcium recording buffer) for 30 min. After loading, cells were incubated in same calcium recording buffer without Fura-2 AM for 20 min. Cells were excited at 340 nm and 380 nm, and Fura-2 AM emission at 505 nm was monitored in Olympus real-time Calcium imaging microscope (FV-1000). Calibration of Fura-2 AM was performed as described (Palmer et al., 2004). Cells were treated with 10 mM ionomycin and 10 mM EGTA in Ca^{2+} free buffer to obtain R_{min} and with 20 mM Ca^{2+} in calcium recording buffer to obtain R_{max}. The standard equation: $K_d[(R-R_{min})/(R_{max}-R)]*S_f/S_b$ was used to convert the Fura-2 AM ratio to cytosolic calcium, where S_f and S_b are the emission intensities at 380 nm for Ca^{2+} free and Ca^{2+}-bound Fura-2 AM, respectively. R_{min} and R_{max} values were multiplied by 0.85 to adjust for the minimum viscosity effect. For quantification of ionomycin-releasable ER Ca^{2+} stores, the integrated Ca^{2+} flux within the 2min after ionomycin treatment was calculated using the summation of $([R_n/R_0]-1)$; R is the ratio of fluorescence intensity upon excitation at 340 nm to that upon excitation at 380 nm, n is the number of measurement, R_0 is the background intensity ratio, and R_n is the fluorescence intensity ratio at time point n.

Immunohistochemistry

Immunohistochemistry of mito-GFP in *Drosophila* brain was performed as described (Wu et al., 2013). The primary antibodies used were: chicken anti-GFP (1:2000; Abcam), mouse anti-Eyeless (1:1000), mouse anti-Pros (1:200) and mouse anti-NICD (1:100; Developmental Studies Hybridoma Bank [DSHB]), guinea pig anti-Dpn (1:1000; J. Skeath), rabbit anti-Dpn (1:1000; YN Jan), guinea pig anti-Dichaete (1:500; J. Nambu), anti-Miranda (1:500; YN Jan), rabbit anti-TH (1:500), Guinea pig anti-dMiro (1:500; K Zinsmaier), pS66-dMiro (1:200), Rhot1 (1:200), KDEL (1:200, Chemicon), pPDHE1

(1:200, Millipore), Caspase-3 (1:100, Cell Signaling), p-eIF2alpha (1:100, Cell Signaling), ATPsyn5α (1:500, abcam), Calnexin (1:200, abcam), Myc (1:1000, Santa Cruz). All secondary antibodies (Molecular Probes) and Texas Red or FITC-conjugated anti-HRP (Jackson ImmunoResearch Laboratories) were used at 1:200 and incubated for about 2 hours at room temperature. Laval preparations were mounted in SlowFade Antifade kit (Invitrogen).

Measuring Mitochondrial Membrane Potential

Third instar level brains expressing mito-GCaMP3.0 were dissected and treated with 100 nM TMRM (Tetramethylrhodamine methyl ester perchlorate, Sigma) in 0.1% PBST for 1 hr at room temperature. After treatment with TMRM, brains were mounted in 1X PBS. As a control, 20 μM CCCP was applied for 1 hour on the same brain samples under the coverslip. Images were taken with a Leica TCS SP5 AOBS confocal microscope equipped with a laser scanner and a 40x oil-immersion objective. Series of z-stack images of the larval brain (step size of 0.5 μm) were taken (1024x1024 pixel; pinhole 1AU; 1x digital zoom), and processed under identical conditions in Photoshop.

Measurement of Mitochondrial Oxygen Consumption Rate (OCR) and Glycolytic Rate (ECAR)

The mitochondrial OCR was determined using a XF-24 analyzer (Seahorse Biosciences). ReN cells were plated in a XF 24 cell culture microplate. The next day, the cells were incubated with low-glucose (1 mM) medium overnight and the sensor cartridge was hydrated overnight according to the manufacturers' instructions. Measurements were performed 48 h after transfection. The measured values were normalized to protein levels. The cells were washed using the XF Prep Station three times with Seahorse Medium containing 10 mM galactose and 1 mM pyruvate. Mitochondrial function was analyzed using the XF Cell Mito Stress Test Kit (Seahorse Biosciences) and all measurements were carried out at 37°C. The following drugs were diluted in Seahorse Medium and loaded onto the sensor cartridge: oligomycin, carbonyl cyanide p-(trifluoromethoxy) phenylhydrazone (FCCP), and rotenone. The drugs

were diluted in Seahorse Medium and loaded onto the sensor cartridge. Measured values were normalized to protein levels.

For measuring glycolytic rate (ECAR), cells in a XF 24 cell culture microplate were incubated for 24 hr before the assay. The media was changed to DMEM (without serum, glucose or bicarbonate, but with 2 mM Glutamine). Injections of 10 mM glucose, 3 μM oligomycin and 0.1 M 2-DG were diluted in the DMEM media and loaded onto ports A, B and C respectively. The assay was repeated at least 3 times.

Statistical Analysis:

Statistical significance of all data were evaluated by unpaired Student's *t*-tests. Error bars represent standard error of the mean (SEM).

Supplemental References

Feng, M., Grice, D.M., Faddy, H.M., Nguyen, N., Leitch, S., Wang, Y., Muend, S., Kenny, P.A., Sukumar, S., Roberts-Thomson, S.J.*, et al.* (2010). Store-independent activation of Orai1 by SPCA2 in mammary tumors. Cell *143*, 84-98.

Lutas, A., Wahlmark, C.J., Acharjee, S., and Kawasaki, F. (2012). Genetic analysis in Drosophila reveals a role for the mitochondrial protein p32 in synaptic transmission. G3 *2*, 59-69.

Palmer, A.E., Jin, C., Reed, J.C., and Tsien, R.Y. (2004). Bcl-2-mediated alterations in endoplasmic reticulum Ca2+ analyzed with an improved genetically encoded fluorescent sensor. Proc Natl Acad Sci USA *101*, 17404-17409.

Song, Y., and Lu, B. (2011). Regulation of cell growth by Notch signaling and its differential requirement in normal vs. tumor-forming stem cells in Drosophila. Genes Dev *25*, 2644-2658.

Wu, Z., Sawada, T., Shiba, K., Liu, S., Kanao, T., Takahashi, R., Hattori, N., Imai, Y., and Lu, B. (2013). Tricornered/NDR kinase signaling mediates PINK1-directed mitochondrial quality control and tissue maintenance. Genes Dev *27*, 157-162.